# Assessment of H&CD System Capabilities for DEMO

[1]H. Zohm, [2]E. Barbato, [3]I. Jenkins, [3]R. Kemp, [4]E. Lerche, [1]E. Poli, [1]G. Tardini, [4]D. v. Eester

*[1]MPI for Plasma Physics Garching, Germany, EURATOM Association*
*[2]ENEA Frascati, Italy, EURATOM Association*
*[3]CCFE Culham, United Kingdom, EURATOM Association*
*[4]LPP-ERM/KMS, Brussels, Belgium, EURATOM Association*

**Introduction:** Studies for DEMO, the step after ITER, indicate that substantial current drive may be needed if steady state operation is envisaged at realistically achievable bootstrap fraction. Since DEMO will be a point design, optimization of H&CD systems may follow a different route than for ITER. In this contribution, we assess the capabilities of 4 candidate systems, namely ICCD, ECCD, LHCD and NBCD, for CD in an 'Early' DEMO, i.e. a design based on moderate extrapolation of ITER physics and technology assumptions [1].

**Methodology:** Starting point of the analysis for the Early DEMO was a 0-d parameter set from the PROCESS code [2] ($R_0$=9 m, a = 2.25 m, $I_p$ = 14 MA, $n_{e,lav} = 8.8 \times 10^{19}$ m$^{-3}$, $\beta_N$ = 2.2, leading to $P_{fus}$ = 1.6 GW and $P_{el,net}$ = 500 MW). Since CD calculations critically depend on kinetic profiles, The 0-d PROCESS design point was converted into a set of profiles using the TRANSP and ASTRA transport codes such that they reproduce the 0-d quantities (e.g. line-averaged density, stored energy and fusion power) when integrated over the volume. We have used two sets of profile assumptions, mainly differing in the shape of the density profile. This reflects our uncertainty about the peaking of the density profile: while present day machines usually encounter flat density profiles close to $n_{GW}$, recent analysis has shown that the peakedness of the density profile can well be described in terms of collisionality. Since DEMO will run at high Greenwald fraction, but low collisionality, we have created two sets of profiles representing these two situations. For the impurity profiles, we have used $f_Z = n_Z/n_e$ = const, using the same impurity species as in PROCESS and matching the $Z_{eff}$ value. The peaked density profile is derived by setting the density to the line averaged value at the pedestal top and from there on, the gradient is used consistent with a simulation based on first principles theory [3]. The temperature profile used does not exceed a critical gradient R dT/dR of around 7 at half radius, consistent with the theoretical expectation at $T_e = T_i$ (i.e. substantial ion heat flux). The pedestal temperature is 8.5 keV, consistent with a recent pedestal scaling using ASDEX Upgrade, DIII-D and JET data [4]. In the second set of profiles, the density is essentially flat so that the pedestal value is close to the core value. In this case, the temperature has to be higher on average to match the $\beta_N$-value. Both sets of profiles are shown in Fig. 1.

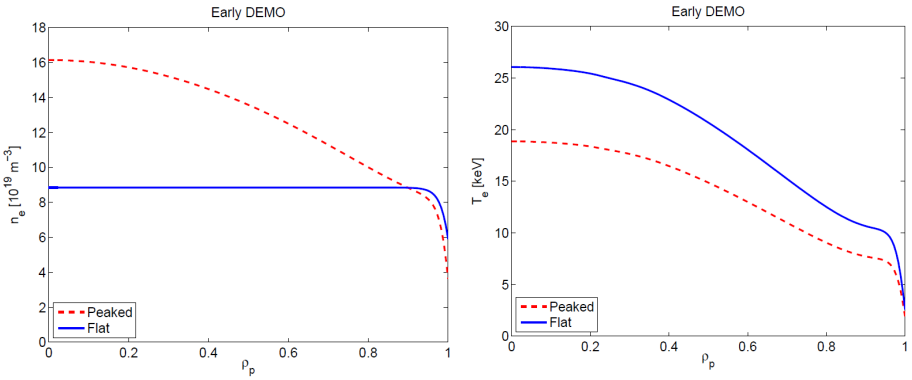


*Fig. 1: Density (left) and temperature (right) for the Early DEMO.*

For localised current drive, a simple figure of merit is the local current drive efficiency

$$\gamma_{CD} = n_e(\rho)\, R_0\, I_{AUX} / P_{CD}(\rho) \qquad (1)$$

($R_0$: major radius, $n_e(\rho)$: local density at $\rho=\rho_{dep}$ where the localized current $I_{CD}$ is driven with power $P_{CD}(\rho)$). For NBI, where the deposition is less localized, we used $\rho=\rho_{tang}$, the radius of

the innermost flux surface reached by the particular NBCD beam. To control the q-profile, the current must be driven with a certain radial distribution to replace the ohmic component of a given current profile. Targeting an 'improved H-mode' regime, we chose a q-profile with q > 1 everywhere and flat q in the core. Different from the local CD efficiency defined in Eqn. (1), we now obtain a 'global' CD efficiency

$$\langle\gamma_{CD}\rangle = n_{e,lav}\, R_0\, I_{AUX} / P_{CD} \qquad (2)$$

for driving a desired current distribution j(ρ). These studies neglect $P_{CD}$ in the power balance and hence do not couple the q-profile to transport. Since the power to drive $V_{loop}$ to zero is not negligible w.r.t. fusion power, we will take into account $P_{CD}$ in the power balance in future.

**Results - ICRH:** Two different frequency windows were studied, one in the classical frequency range around low harmonics of the cyclotron frequency (25-100 MHz) and one corresponding to higher frequencies (High Harmonic Fast Wave Current Drive HHFWCD, 100-350 MHz) [5]. In the 25-100 MHz range, the frequency has to be tailored to avoid 'parasitic' absorption, e.g. by the ions when close to the ion heating scheme. CD efficiency is found to decrease with $k_{||}$ and with $Z_{eff}$. Results indicate good local central CD efficiency for the flat density case at 72 MHz with $\gamma$ = 0.26-0.32 at $Z_{eff}$ = 1.6, depending on the spectrum. Alternatively, a value of $\gamma \approx 0.23$ is found for 25 MHz in the flat density case. Note that the $\gamma$-values quoted here refer to absorbed power and do not take into account coupling issues which largely depend on the assumptions on the SOL profiles.

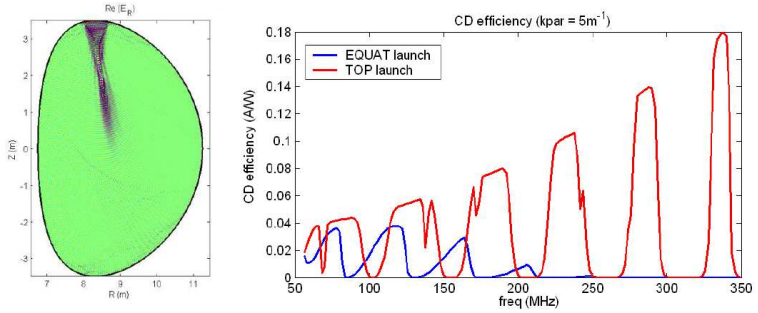


*Fig. 2: top launch HHFWCD ICRH geometry (left) and resulting CD efficiency, compared to equatorial launch.*

For the high frequency window, the main parasitic absorption is on α-particles at various cyclotron harmonics as the HHFWCD wave travels from the midplane launcher to the plasma centre. Studies were hence undertaken to launch HHFWCD from the top of the machine to avoid resonant damping on α-particles. Fig. 2 shows an example. Windows exist in which the parasitic absorption is practically zero, allowing to take advantage of the higher CD efficiency with increasing frequency if good coupling can be realized. Studies have been conducted aiming at central CD, but off-axis CD seems possible as well by adequately tailoring the absorption profile. Future studies will try to clarify the feasibility of this approach and better characterize its benefits.

**ECRH:** The TORBEAM code [6] was coupled to the ASTRA transport code and benchmarked in the fully relativistic, momentum conserving approach against GRAY [7], yielding good agreement. For the Early DEMO profiles, scans of the ECCD frequency, together with toroidal and poloidal launch angle to control the deposition location, show an increase in CD efficiency with frequency, but this effect is limited by parasitic 2nd harmonic absorption. Top launch can circumvent this problem [8]. For the flat density case, a maximum local CD efficiency of $\gamma_{CD}$ = 0.41 has been obtained using top launch at 280 GHz and on-axis deposition. Reducing the frequency to 250 GHz, in order to ease the technology requirements, results in $\gamma_{CD}$ = 0.34. By scanning the launch angles, current can be driven almost anywhere in the plasma, albeit at reduced efficiency w.r.t. the on-axis case since ECCD efficiency roughly scales with $T_e$. Typical $\gamma$ values for the flat density case are of the order of 0.25-0.35 for off-axis at roughly half radius using 280 GHz. An advantage of ECCD over the other systems is

that individual beams yield a well-localized driven current profile such that it is also suited for MHD control. Also, by introducing beam steering or frequency tuning, the deposition can be controlled, allowing feedback applications.

**LHCD:** LHCD is evaluated using the FRTC ray tracing Fokker-Planck code [9]. The analysis was conducted in a way where ASTRA takes into account the change in current profiles due to ECCD self-consistently. LH waves were launched at $N_{||}$ = 1.8 and 5 GHz. For both peaked and flat density profiles, the deposition is found to be in the outer part of the plasma since the high temperatures occurring there lead to rather peripheral single pass absorption. For the early DEMO, maxima of the driven current are at $\rho = 0.7$ for the peaked density and $\rho = 0.8$ for the flat density (which has even higher edge temperature). The current drive efficiency is comparatively high there, of the order of $\gamma = 0.3$ which is substantial given the far off-axis location. However, due to the peripheral CD, LHCD cannot be used alone to replace an arbitrary ohmic current profile in the Early DEMO.

**NBCD:** For NBCD, TRANSP is the reference analysis code due to the quite complete physics description. However, a PENCIL code is used for rough scoping studies, in particular for an iteration loop that has been set up to find an NBI geometry that, for given kinetic profiles, can synthesize $j_{NBI} = j_{tot}\text{-}j_{BS}$ [10]. This module has been used in current profile control studies to replace the ohmic current. No effort has been made so far to achieve consistency of the NBCD source geometry obtained from the optimization process with the machine boundary conditions, but it is expected that this can be achieved with some trade-off in efficiency.

NBCD analysis for the flat density case assuming a beam energy of 1.5 MeV shows good central CD efficiency, in the range of $\gamma = 0.3\text{-}0.45$. A particular strength of NBCD is that $\gamma$ does not drop when going to off-axis CD since the negative effect of the decrease in $T_e$ is (over)compensated by a larger trapped electron fraction beneficial for NBCD. This leads to a net increase of $\gamma$ when moving to off-axis NBCD. Hence, NBCD is very well suited to synthesize a given current profile. On the other hand, there is little flexibility in changing this profile assuming that the beam geometry and the plasma scenario are fixed.

**Results for current profile control:** Here, we analyse how the ohmic current can be replaced by NBCD or ECCD (for ICCD and LHCD no such attempt was made due to the limited flexibility in deposition). For the ECCD case, power was deposited at three locations with Gaussian profile until a consistent solution with $q_{min} \geq 1$ was reached. Hence, the match with the initial q-profile is not perfect and cannot be considered as a rigorous optimization, and we note that a better match may increase the requirements due to more off-axis power to keep the q-profile above 1 there. In the example shown in Fig. 3, 10.4 MA are driven with 293 MW of ECCD, resulting in an averaged efficiency (see Eqn. 2) of $\langle\gamma\rangle = 0.3$. For the peaked density, using 270 GHz, the substantially lower temperature leads to a reduction, $\langle\gamma\rangle = 0.17$. Based on the findings for local $\gamma$ quoted above, we expect that reducing the frequency to 250 GHz to ease technology requirements will reduce $\gamma$ by about 20%.

For NBCD, an optimization using the algorithm outlined in the previous section leads to a stationary solution applying 250 MW to drive 11.3 MA, the slightly different values of $I_{CD}$ coming from a different bootstrap fraction. This leads to a value of $\langle\gamma\rangle = 0.35$, in line with the findings of higher off-axis CD efficiency than ECCD discussed in the previous section. Fig. 3 shows the driven current profile resulting from the optimization process for the flat density case, together with the distribution of tangency points and inclination angles of the different beam sources used to drive it. For the peaked density case, the figure of merit drops to $\langle\gamma\rangle \sim 0.21$. Reducing the beam energy to 1 MeV to account for technology constraints, the CD efficiency drops to $\langle\gamma\rangle = 0.28$ for flat density and $\langle\gamma\rangle = 0.19$ for peaked density.

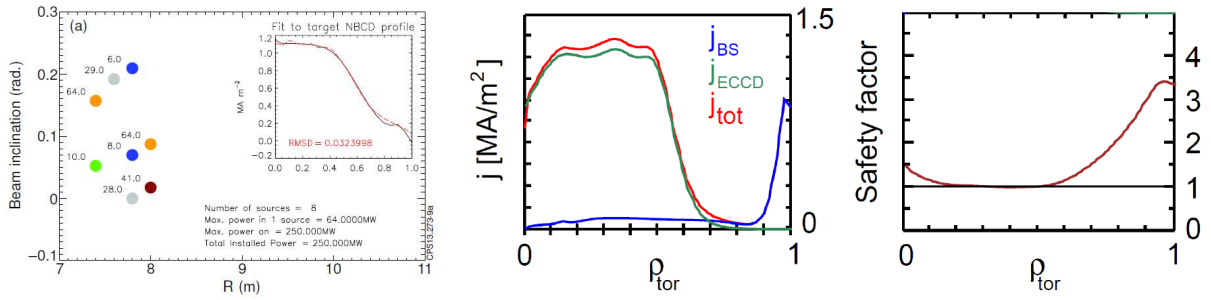


*Fig 3: NBCD (left) and ECCD driven current (middle) and q-profile (right) for the flat density case.*

In summary, both ECCD and NBCD can synthesize the required current profile, with NBCD being more efficient by about 20-30%, depending on the exact shape of the q-profile. While optimization of both cases will be required to incorporate technical boundary conditions such as available gyrotron frequencies, beam energies and the restrictions on launch geometry, the results can still be taken as indicative of the potential of both methods for DEMO.

**Summary and Conclusions:** Local analysis of the CD capabilities of H&CD systems for an Early DEMO shows that ICCD is mainly suited for central CD, while LHCD can exclusively drive far off-axis ($\rho > 0.7$) current for the profiles studies. Due to the constrained radial range, both systems cannot be used to individually synthesize the ohmic contribution to the current profile. ECCD and NBCD are more flexible and can synthesize the desired current profile. The results are summarized in Table 1.

| local $\gamma_{CD}$ | ICCD | LHCD | NBCD | ECCD |
|---|---|---|---|---|
| central | 0.23-0.32 | - | 0.3-0.45 | 0.35-0.4 |
| off-axis | - | 0.3 | 0.4-0.55 | 0.25-0.3 |
| remark | $Z_{eff}$ corrected | r=0.7 | r=0.4 | r=0.4 |
| global $\gamma_{CD}$ | ICCD | LHCD | NBCD | ECCD |
| DEMO1, flat | n/a | n/a | 0.35 | 0.3 |
| DEMO1, pkd | n/a | n/a | 0.21 | 0.17 |

*Table 1: local and global CD efficiencies for Early DEMO.*

In the 0-d modelling with PROCESS, an overall NBCD efficiency of $\langle\gamma\rangle = 0.373$ had been assumed for the flat profile case, very well in line with the numbers found above. In an earlier study of an 'advanced' DEMO, numbers quoted for NBCD are 0.45 at 1 MeV and 0.5 at 1.5 MeV [11]. For ECCD, that study suggested a value of 0.2, while our optimisation suggests that higher values are possible. From the large spread of values caused by different density profiles, it follows that DEMO designs have to be optimized taking into account the individual strengths of H&CD systems from the beginning, especially for designs aiming at steady state.

## References


[1] G. Federici et al., SOFE Conference, San Francisco (2013)
[2] P. J. Knight, 'A User Guide to the PROCESS Systems Code', rev. 178 (2013), CCFE
[3] G. Pereverzev et al., *Nucl. Fusion* **45** (2005) 221
[4] P.A. Schneider et al., *Plasma Physics and Controlled Fusion* 54, 10 (2012), 105009
[5] D. v. Eester et al., RF Conference, Sorrento (2013)
[6] E. Poli et al, Comp. Phys. Comm **136** (2001), 90
[7] D. Farina et al., Fus. Sci. Technology **52** (2007) 154
[8] E. Poli et al., Nucl. Fusion **53** (2013) 013011
[9] E. Barbato et al., Plasma Phys. and Control. Fusion **46**, (2004) 1283.
[10] I. Jenkins et al., SOFE Conference, San Francisco (2013)
[11] J. Garcia et al., Nucl. Fusion **48** (2008) 075007